A Database for Storing Magnet Parameters and Analysis of Quench Test Results in HL-LHC Nb3Sn Short Model Magnets

A Database for Storing Magnet Parameters and Analysis of Quench Test Results in HL-LHC Nb_3Sn Short Model Magnets

T. Salmi[1], T. Tarhasaari[1,2] and S. Izquierdo-Bermudez[3]

***Abstract*— In recent years, several Nb_3Sn high field magnet prototypes have been designed and tested in preparation for the LHC Luminosity upgrade and also for the potential Future Circular Collider (FCC). In this paper we present a Microsoft Excel -based database tool for storing magnet design parameters and results from quench protection tests. The hierarchical and flexible structure of the relational database allows for systematic and coherent analysis of the test data from different magnet assemblies and works as a practical reference for magnet design evolution. Data from quench protection heater tests in several high-field Nb_3Sn magnet prototypes has been stored in the database. We use this data to validate the quench simulation assumptions used in FCC 16 T dipole magnet design.**

***Index Terms*—Superconducting magnets, quench protection, quench protection heaters.**

I. Introduction

Future high-energy particle accelerators and upgrades of existing accelerators such as the LHC at CERN require superconducting magnets with higher magnetic fields to control the paths of the high energy particles [1-3]. The higher magnetic field leads to higher stored energy density, which implies increased challenge for the quench protection: A faster discharge of the magnet current is required to avoid overheating due to resistive losses if the superconducting state is locally lost [4-5]. The fast discharge is obtained by bringing the entire winding into normal state, thus increasing the circuit resistance and enabling uniform dissipation of the energy within the windings. The protection of the present LHC NbTi dipoles is based on quench heaters which heat a large fraction of the coil above the critical temperature [6]. The protection of the Nb_3Sn dipoles for the High-Luminosity LHC (HL-LHC) will be based on heaters and a combination of heaters and the novel CLIQ system in the quadupoles [7-9].

The development of the magnets and protection systems involves computational studies and experimental works on the various prototype magnets. The experiments are rather expensive and typically only a few tests are made for each magnet. For HL-LHC, experiments at different laboratories have been made for over a decade, and now a larger amount of data has been accumulated.

[1]T. Salmi is with Tampere University, FI-33101 Tampere, Finland (e-mail : tiina.salmi@tuni.fi). [1,2]T. Tarhasaari was with Tampere University and is now with Jalonne, 33100, Tampere, Finland. 3S. Izquierdo-Bermudez is with CERN, 1211 Geneva, Switzerland. Manuscript received 24th September 2019. This work was supported by CERN under the FCC addendum (FCC-GOV-CC-0067) and Academy of Finland (QuenchCirCol, Grant 295185).

In this paper we present a database tool for collecting and summarizing the experimental results, regardless of the test location. It ensures that the needed data is systematically collected and that comparable data can be selected for analysis. The focus is on the quench heater tests, thus the analysis of heater delays and coil resistance development after heater firing. The structure of the database is flexible so that in future also other type of tests, such as CLIQ tests and training quenches, can be stored. We have analyzed data from quench heater tests in 8 HL-LHC Nb_3Sn magnets tested at CERN in recent years. The experimental data is previously analyzed and published as detailed in the manuscript, but with the systematic re-analysis we ensured consistent interpretation methodology for measurements stored in the database.

The stored experimental data on quench heater delays and coil resistance increase has been used to validate the simulation models and assumptions that were used in the quench protection design for the 16 T dipoles for the Future Circular Collider [10]. After the database tool description, we proceed in discussing the experimental uncertainty in the heater delays, as well as the difference when compared to simulated delays. Then we compare the measured magnet resistance increase and current decay to simulations and discuss different ways to model the Rutherford cable. The simulation models are the same as used the EuroCirCol FCC 16 T dipole magnet design.

II. Quench Protection Database (QPDB) tool

The Quench Protection Database (QPDB) is built in Microsoft Excel utilizing VBA-macros and -functions. The tool consists of two Excel files: The data-file (DB) and the user interface (UI). Through the UI the user can access, modify, select and extract experimental data that is stored in the DB.

A. Structure of the relational database

QPDB is a relational database where items can be linked to each other, see Fig. 1. The idea is similar to the commonly used accelerator magnet design tool ROXIE input [11], where items such as filaments and cable geometries are defined independently, and then linked to the defined coil cross-section. In QPDB each item is represented as a table in its own sheet. The VBA functions programmed in the UI follow the links defined in DB, and connect the right parameters to each magnet and to each measurement. The tables are designed to account all parameters which are relevant for quench tests. However, the structure is flexible and the tables can be modified in the future, if needed. Details of the stored parameters can be found in the user manual [12].

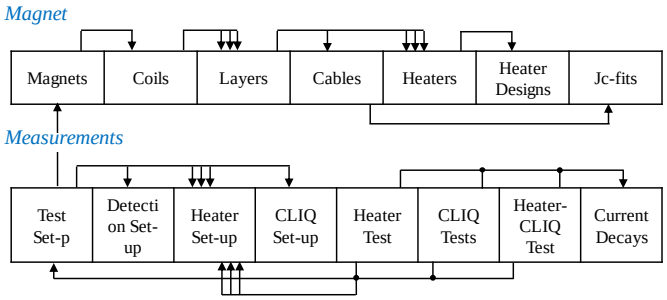

Figure 1: A schematic of the database structure. Data is divided into two categories: *Magnet*, for magnet design parameters, and *Measurements*, to describe the test set-up, and the results from quench protection tests. The arrows indicate links between tables. A triple-arrow indicates that each item can be connected to several items in the target table, for example a coil can be connected to several layers.

B. *Internally computed quantities*

The UI is used to fill the DB with measured parameters, or design values. Internal VBA functions subsequently compute several derived quantities based on the input data. For example, cable cross-sectional areas, critical current and temperature, magnetic field, heater delay, and coil resistance are computed automatically. If one input parameter is updated, the needed modifications propagate automatically in the DB.

The current decay after quench is stored as a piecewise polynomial fit, which allows automatic computation of quench load, i.e., MIITs [4], for various time intervals. An appended Matlab function is provided for fitting the polynomials directly from measured current decay. All computed quantities are detailed in the user manual [12].

III. Stored Heater Delay Measurements

A. *Magnets and heater designs*

The analyzed magnets within this paper are the HL-LHC short model quadrupoles MQXFS3a, MQXFS3b, MQXFS5a, and the 11 T dipole models SP101, SP103, SP105, SP106 and DP101. Detailed magnet design and previous analyses can be found in [7-8] [13-15].

All the magnets feature quench heaters. The quench heaters have periodical stainless-steel heating stations, separated by low-resistance copper plating [16-17]. The 11 T and MQXFS5a models have heaters only on coil outer layer (OL). The MQXFS3 models had heaters connected also on the inner layer (IL). In MQXFS models the heater strips on coil high-field (HF) and low-field region (LF) could be individually tested.

B. *Uncertainties in the measurements*

Heater delay is measured by firing one or more heater circuit and defining quench onset from the measured coil voltage. If the magnet current is close to the short sample limit, the time instant of the first resistive transition is clearly visible. At lower currents, the cable resistance increases slower, and current and magnetic field redistribution obscure the quench onset time [18-19]. This *reading uncertainty* is accounted in the database by storing an error bar quantifying the ambiguity, or the confidence interval, in definition of each quench onset time.

The *reproducibility uncertainty* describes the variation of the result when the measurement is repeated. We include here the variation of the delay in different coils and heaters if they are fabricated using the same specifications.

Average uncertainty is associated to the average delay at each current. It is defined as the average of the *reading uncertainty* (for each measurement choose the larger of the upper and lower error bars), added with the average absolute deviation of the quench onsets within the set of measurements at that current. The *average uncertainty* for the stored heater delay measurements is shown in Fig. 2. It is typically 2 ms, or 15-20%, at nominal current. At lower current the error varies from 5 to 40% in different magnets and heaters, the average still being around 20%. In the cases of MQXFS LF and IL heaters only one measurement was done. More statistics are needed to make this a fully useful parameter.

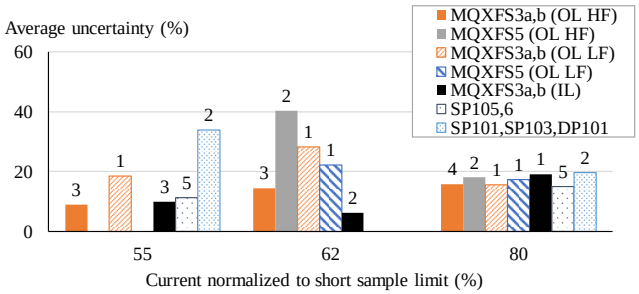

Figure 2: Summary of average uncertainties related to measurements in each magnet. The number of repeated measurements in each case is marked.

C. *Comparison with simulation*

Heater delay simulation is done with the 2-D heat diffusion computation model CoHDA [19]. It computes the heat diffusion from the heater to the cable trough the various insulation layers. This method was used in the design of the HL-LHC heaters. Fig. 3 and 4 summarize the simulation delays and comparison to the measurements.

As in the previous analyses, the agreement between measurement and simulation is good, especially near the operating current. At lower current, both the experimental uncertainty and disagreement with the simulation increase. The longer delay time leads to more uncertainty due to increased cable heat capacity, decaying quench heater power, effect of current redistribution in the cable, and uncertainty in the critical surface parameterization [18]. Fortunately, the low current regime is not as critical for the heater-based quench protection design as the high current regime.

Significant (>20%) difference between simulation and measurement are found only for the MQXFS3 LF heater at nominal current, IL heater at lower than nominal current, and for the 11 T SP105 and SP106 simulation. The IL heater tends to detach from the coil surface, thus the longer than simulated delay is expected. The LF heater case will be studied after more measurements. These results supported the choice of 20% heater delay uncertainty margin in the FCC quench protection design.

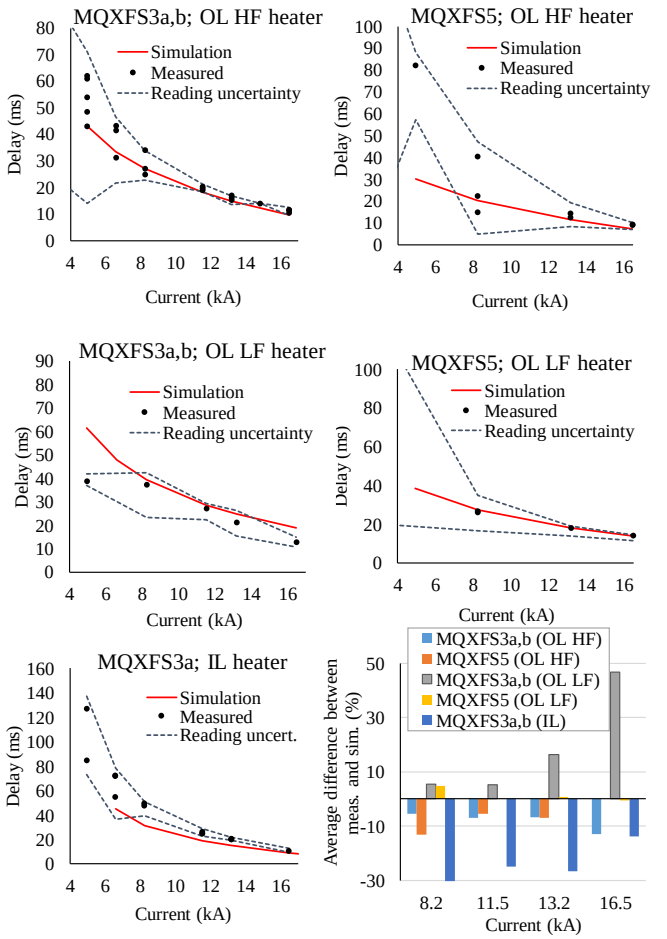

Figure 3: Summary of heater delays in MQXFS models, and the difference between simulation and measurement. The maximum reading uncertainty associated with the measurement at each current is shown.

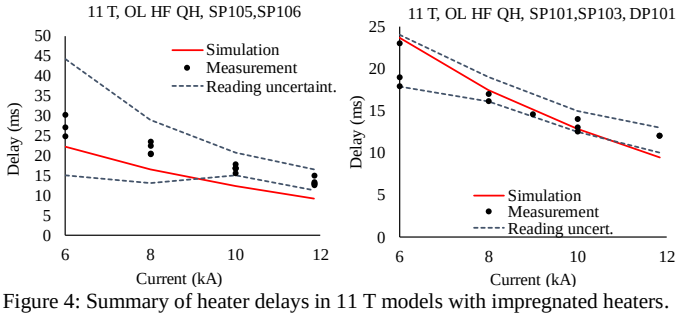

Figure 4: Summary of heater delays in 11 T models with impregnated heaters.

IV. Coil Resistance Increase and Current Decays

Only the first heater delay can be deduced from the coil voltages. To understand how the heaters quench the rest of the coil, one needs to measure the magnet resistance build-up. The magnet resistance can be derived based on the current decay and inductance (L), assuming an exponential current decay with time constant $R(t)/L(t)$ between each time step, Δt.

$$R(t) = -\frac{\ln\left(\frac{i(t+\Delta t)}{i(t)}\right) L(i)}{\Delta t}. \qquad (1)$$

The differential inductance as a function of current, $L(i)$, is based on computation with ROXIE [11]. Analyses of the coil resistance evolution and heater efficiency is already presented in [16-17] [20-21]. This section focuses on comparison of the data with the simulation models that were used for the FCC magnets.

A. Simulation models

The magnet resistance increase and current decay is simulated using the tool Coodi [22]. Coodi takes as an input the quench heater delays, which are simulated using CoHDA, and quench propagation velocities in each coil turn. It computes adiabatically the temperature and resistance increase at each time step, and subsequently the magnet current decay. At nominal current the input longitudinal quench propagation velocity is 18 m/s. The turn-to-turn quench propagation time is 11 ms and propagation time from outer layer to inner layer is 22 ms. At lower currents, the propagation slows down proportionally to the square of the current.

In the quenched cable the current flows only in the copper stabilizer. In the keystoned Rutherford cable the twisted strands are tightly pressed against each other. Depending on the electrical contact resistance between the strands, the current can either follow the strand path, or flow as if the cable copper surface was one straight conductor. Fig. 5 shows the different possible cases how the current flow can be simulated.

In many previous quench models the twisting of the strand have been neglected (Case A). In the first EuroCirCol simulations, the twisting was accounted in the copper cross-sectional surface area, but the longer current path for quenched cable was not accounted (Case B) [22]. The simulations were then updated to correspond a case with twisted strand and no current sharing between strands (Case C) [10]. Also coil room temperature measurements agree best with this case.

Material properties for cable are in [10]. The impact of simulating the voids between strands either with G10 or epoxy is investigated.

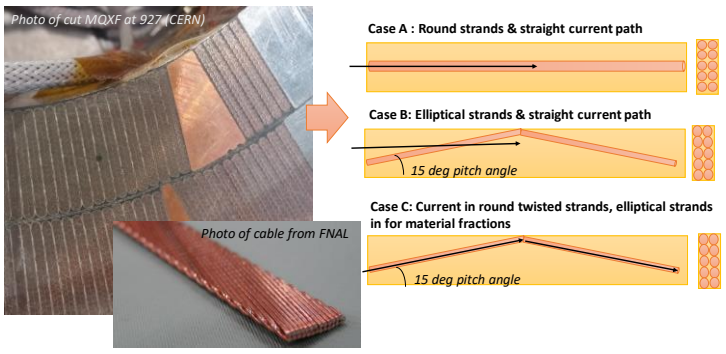

Figure 5: Three cases how the current flow in quenched cable can be simulated.

B. Impact of the different cable simulation methods

The different cable simulation methods was investigated for the case when both inner and outer layer quench heaters were activated in MQXFS3b. Fig. 6 shows the simulated quench delays at nominal operation current. It includes the turn-to-turn quench propagation to the coil turns, which are not covered by heaters. Two IL heater strips were disconnected during the test, and this is accounted in the simulation. The impact of disconnected heater strips was quantified by repeating the

simulation with all strips connected. Fig. 7 shows the computed and measured coil resistance evolution in the different cases at nominal current (with disconnected strips and cable voids filled with G10).

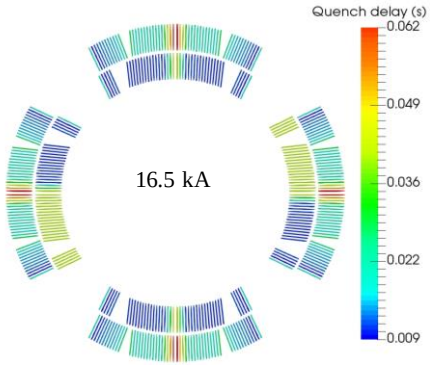

Figure 6: Simulated heater delays in MQXFS3 at nominal current when two inner layer heater strips are disconnected.

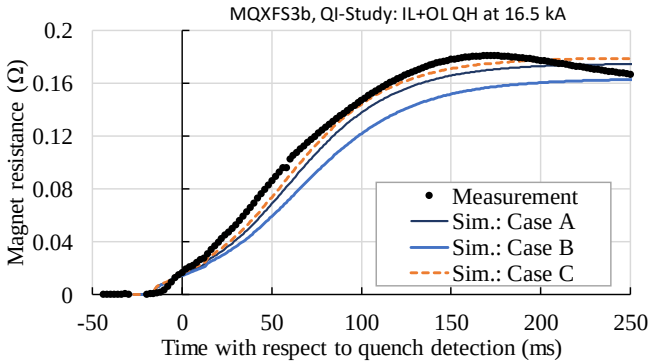

Figure 7: Measured magnet resistance in MQXFS3b after OL and IL heater activation compared with different simulation scenarios.

The Case C simulation has the best agreement with the experiment. A good agreement in current decay directly follows from the good agreement of resistance development. The magnet final resistances and quench load (MIITs) of the current decay are compared in Table I.

Table I: Comparison of final magnet resistances and MIITs in the MQXFS3 simulation with IL and OL quench heaters at nominal current. The MIITs are computed from the moment of quench heater activation.

	R_{max} (Ω)	MIITs (10^6 A^2 s)	ΔMIITs (%)
Measurement	0.180	25.8	
Case A	0.175	27	5
Case B	0.163	28.5	11
Case C	0.179	26.3	2

The difference in MIITs for Case A and C is 3%, but between B and C it is 9%. If the two missing IL strips would have been connected, the simulated MIITs would be lowered by 3% in all cases. The difference between simulating the cable voids with epoxy or G10 properties was only 1%. Case C leads to stronger heating in the coil, thus faster resistance increase and current decay. For a real quench, the hotspot temperature would be higher due to stronger heating during the detection time.

At the beginning of the quench the simulated resistance increased faster than the measured. In the cases where only OL heaters were fired, this difference was not visible. We therefore associate it with the over-optimistic simulation of the inner layer heaters. The inner layer heaters are not anymore in the MQXFS protection baseline. Towards the end of the current decay (after 150 ms) the measured resistance starts to decrease. One reason may be that heat starts to diffuse to surrounding components from the strand. The adiabatic simulation cannot reproduce this effect.

C. Current decays in the MQXFS quadrupole

Fig. 8 shows the simulated (Case C) and measured magnet resistance development when all outer layer heaters are activated at nominal current in MQXFS3 or in MQXFS5. In the simulation the inner layer quenches all at once. Its quench time is the average quench delay in OL added with the layer-to-layer propagation velocity.

The simulated resistance development is in good agreement with the measurement, although in MQXFS5 the simulation slightly underestimates the measurement. The resistance development and current decays also agree well also at lower currents, as summarized in Fig. 9. The resistance is not significantly impacted by the heater configuration. On the other hand, in MQXFS3 has significantly higher MIITs than MQXFS5 when only OL heaters are fired. The reason is assumed to be lower RRR.

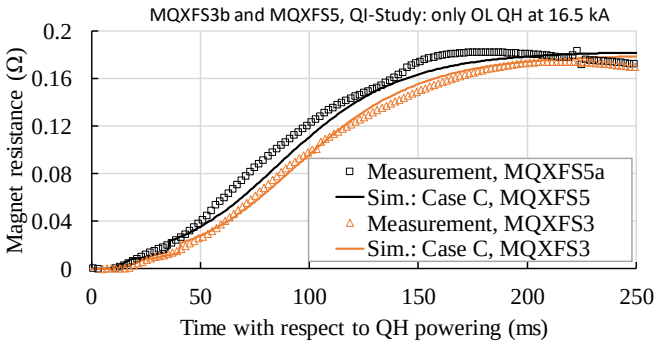

Figure 8: Measured and computed coil resistance in MQXFS3b and MQXFS5 when OL heaters activated at nominal current. The heater peak power is 200 W/cm^2 in MQXFS5 and 110 W/cm^2 in MQXFS3 models.

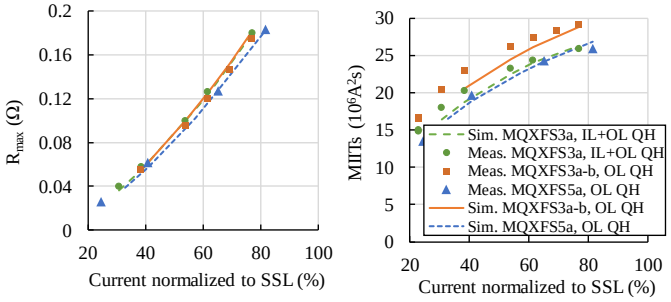

Figure 9: Summary of measured and simulated final magnet resistances and MIITs from MQXS3 and MQXFS5 models. The magnet current is normalized to the short sample limit (21.4 kA).

D. Current decays in the 11 T dipoles

The simulated resistance and current decays in SP105 and SP106 11 T models are compared with measurements. The simulated and measured resistances agreed well at currents 11.8 kA, 10 kA, and 8 kA, as shown in Fig. 10.

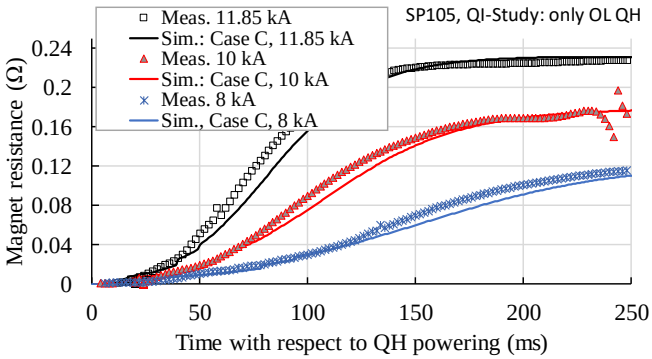

Figure 10: Current decay after OL heater powering in 11 T SP105 and comparison with simulation.

Table II summarizes the measured and simulated final resistance and MIITs from the moment of heater activation. The agreement between simulation and measurement is good: At high current the difference in the MIITs is 3%. The good agreement for both the quadrupole and the dipole magnet gives more confidence to the simulation method.

Table II: Summary of measurement results in 11 T model SP105, after all OL heaters are activated.

I_{mag} (kA)	R_{max} (Ω) *Meas.*	R_{max} (Ω) *Sim*	MIIts (MA^2s) *meas*	MIIts (MA^2s) *sim*
11.85	0.230	0.230	12.34	12.64
10.00	0.176	0.176	11.63	11.78
8.00	0.125	0.123	10.41	10.7

V. Conclusions

The QPDB tool has been designed to store all the magnet and test parameters that are relevant in understanding and reproducing experimental quench protection test results. It is based on interlinked Excel tables and includes several internally computed quantities. In addition of the quench test data, it can be handy in tracking changes between magnet designs and storing simulation results.

Data from several Nb_3Sn quadrupole and dipole magnet tests was analyzed (or re-analyzed) and input into the database. We presented summaries of heater delays, quantified the experimental uncertainties and agreement with simulations. At high current the OL HF heater delays were typically well reproduced by simulations. Simulations tend to underestimate the delays at inner layer and overestimate them at low-field region. One reason for longer than expected delays in IL is the compromised contact of heater with the high field region of the coil.

The data of magnet resistance increase and current decay after protection activation was used to improve and validate the simulation assumptions in the EuroCirCol magnet design. After adjusting the cable simulation method, the agreement between current decay simulation was good.

Acknowledgement

Thanks to the CERN SM18 test facility team for providing data, especially H. Bajas, G. Willering. Thanks to C. Barbagallo (CERN) for participating in the analysis and filling the data for one 11 T model. Thanks to A. Stenvall (TAU) for mentor support during the project.

References

[1] E. Todesco et al., "A First Baseline for the Magnets in the High Luminosity LHC Insertion Regions," *IEEE Trans. Appl. Supercond.,* 24 (3), 2014, *4003305*.

[2] D. Schoerling et al., "The 16 T dipole development program for FCC and HE-LHC", *IEEE Trans. Appl. Supercond.*, 29(5), 2019

[3] Future Circular Collider Study website." [Online]. Available: https://fcc.web.cern.ch/. [Accessed: 16-Jun-2016].

[4] T. Salmi et al., "Quench Protection Challenges in Long Nb_3Sn Accelerator Magnets", AIP Conference Proceedings 1434, pp. 656-663, 2012.

[5] M. Benedikt et al., "Challenges for highest energy circular colliders", Proc. IPAC Int. Conf. Accelerators 2014, and CERN-ACC-2014-0153, 2014.

[6] O. S. Bruning et al., (editors), "LHC design report vol. 1: The LHC main ring", CERN-2004-003, 2004.

[7] E. Ravaioli et al., "Quench Protection System Optimization for the High Luminosity LHC Nb_3Sn Quadrupoles", *IEEE Trans.Appl.Supercond.* 27(4), 2017, *4702107*.

[8] S. Izquierdo-Bermudez, *et al.*," Quench Protection of the 11 T Nb_3Sn Dipole for the High Luminosity LHC" *IEEE Trans. Appl. Supercond.*, 28(3), 2018, 4006405.

[9] E. Ravaioli, CLIQ: A new quench protection technology for superconducting magnets, Ph.D. thesis, University Twente, Faculty of Science and Techology, and CERN, 2015

[10] T. Salmi, M. Prioli, A. Stenvall, AP. Verweij, "Quench Protection of the 16 T Nb_3Sn Dipole Magnets Designed for the Future Circular Collider", *IEEE Trans. Appl. Supercond.*, 29 (5), 2019

[11] S. Russenschuck, "ROXIE : A Computer Code for the Integrated Design of Accelerator Magnets," 6th Eur. Part. Accel. Conf. Stock. Sweden; Cern., pp. 2017–2019, Feb. 1999.

[12] QPDB User manual, to be published

[13] H. Bajas *et al.*, "Test Result of the Short Models MQXFS3 and MQXFS5 for the HL-LHC Upgrade," in *IEEE Trans. Appl. Supercond.*, 28(3), 2018, *4007006*.

[14] G. Willering *et al.*, "Comparison of Cold Powering Performance of 2-m-Long Nb3Sn 11 T Model Magnets," in *IEEE Trans. Appl. Supercond.*, 28(3), 2018, .

[15] F. Savary *et al.*, "Design and Construction of the Full-Length Prototype of the 11-T Dipole Magnet for the High Luminosity LHC Project at CERN," in *IEEE Trans.Appl.Supercond.*, 28(3), 2018, *4007106*.

[16] S. Izquierdo Bermudez *et al.*, "Overview of the Quench Heater Performance for MQXF, the Nb_3Sn Low-β Quadrupole for the High Luminosity LHC," in *IEEE Trans. Appl. Supercond.*, 28(4), 2018, 4008406.

[17] S. Izquierdo Bermudez *et al.*, "Quench Protection of the 11 T Nb_3Sn Dipole for the High Luminosity LHC," in *IEEE Trans. Appl. Supercond*, 28(3), 2018, 4006405.

[18] T. Salmi, et al, "Analysis of uncertainties in protection heater delay time measurements and simulations in Nb_3Sn high-field accelerator magnets" *IEEE Trans. on Appl. Supercond*. 25(4), 2015, 4004212.

[19] T. Salmi, et al., "A novel computer code for modeling quench protection heaters in high-field Nb_3Sn accelerator magnets,"*IEEE Trans. Appl. Supercond.*, 24(4), 2014.

[20] S. Izquierdo Bermudez *et al.*, "Quench Protection Studies of the 11-T Nb3Sn Dipole for the LHC Upgrade," in *IEEE Trans. Appl. Supercond.*, 26(4), 2016.

[21] S. I. Bermudez *et al.*, "Quench Protection Study of a 11 T Nb3Sn Model Dipole for the High Luminosity LHC," in *IEEE Trans. Appl. Supercond.* 29(5), 2019, 4701005.

[22] T. Salmi, et al., "Quench protection analysis integrated in the design of dipoles for the Future Circular Collider", *Physical Review Accelerators and Beams* 20 3, 2017, 032401.